Iron-containing materials FeM (M = B, Cr, Ti or VN) prepared by self-propagating high-temperature synthesis

Maxim V. Kuznetsov,*[a] Yury G. Morozov,[a] Inna P. Borovinskaya,[a] Yuri M. Maximov,[b] Ivan P. Parkin[c] and Quentin A. Pankhurst[d]

[a] *SHS Research Centre, Institute of Structural Macrokinetics and Materials Science, Russian Academy of Sciences, 142432 Chernogolovka, Moscow Region, Russian Federation. Fax: +7 095 962 8025; e-mail: kvin@kuznetsov.home.chg.ru*
[b] *Department of Structural Macrokinetics, Tomsk Scientific Centre, Siberian Branch of the Russian Academy of Sciences, 634050 Tomsk, Russian Federation. Fax: +7 3822 25 9838; e-mail: maks@fisman.tomsk.su*
[c] *Department of Chemistry, University College London, London WC1H OAJ, UK. Fax: +44 (0) 20 7679 7463; e-mail: i.p.parkin@ucl.ac.uk*
[d] *Department of Physics and Astronomy, University College London, London WC1E 6BT, UK. Fax: +44 (0) 20 7679 1360; e-mail: q.pankhurst@ucl.ac.uk*

10.1070/MC2002v012n01ABEH001523

The title iron-containing compounds were prepared, and their structural, magnetic and Mössbauer characteristics were examined.

Iron-containing alloys FeM are widely used as individual compounds or the components of cermets and composite materials because of their high wear resistance, thermal stability, hydrogen capacity *etc*.[1–3] FeB and FeCr are components of hard refractory cermet materials [FeCr–TiC and FeAl–(30–90 vol.%) FeB], which have improved abrasive wear properties and can operate at elevated temperatures.[4] Intermetallic compounds of titanium with iron group elements (FeTi) exhibit attractive construction properties, specific durability, plasticity, corrosion resistance and unique shape memory properties.[5] Particular properties of FeV alloy are responsible for its use as protective coatings in sodium- and lithium-cooled nuclear reactors.[6] For the additional protection and improvement of alloy surfaces, for example, nitridation in ammonia can be carried out at 700 K for 24 h.

Metals (Fe, R-10; Cr, PCM and Ti, PTOM) and non-metal (B) powders of ≥ 98% purity and metals oxides of ≥ 99.5% purity were used. All manipulations were carried out in a box filled with argon to prevent oxidation. All self-propagating high-temperature synthesis (SHS) reactions were carried out in an inert atmosphere using dry powders pressed as cylindrical samples (d = 10 mm, h = 20 mm). Ignition operations were made by REKROW (RK-2060) (UK). X-ray powder diffraction was performed in a reflection mode on a Philips X-pert diffractometer (Netherlands) using unfiltered CuKα radiation (λ_1 = 1.5405 Å, λ_2 = 1.5443 Å). Phases were identified and indexed using the JCPDS database and the ASTM and Unit Cell programs. Pycknometric densities were measured by standard methods using toluene; magnetic characteristics were investigated using EG&G PARC 4500 (USA) at room temperature and applied fields up to 10 kOe. SEM/EDAX were determined on JEOL EMA instrument (Japan). ^{57}Fe Mössbauer spectra were recorded on a Wissel MR-260 constant acceleration spectrometer with a triangular drive waveform.

All FeM (M = Cr, Ti or V) compounds were synthesised using the same reaction scheme involving preparation of an initial mixture of individual powders in the ratio 1:1. The general reaction scheme is:

$$Fe + M \longrightarrow FeM \quad (I)$$

The iron–boron alloy may be synthesised by different ways involving combustion in an appropriate mixture of iron(III) oxide and boron powder in an argon atmosphere:

$$Fe_2O_3 + 4B \longrightarrow 2FeB + B_2O_3 \quad (II)$$

The iron–boron alloy can also be produced by parallel reactions in a mixture of iron(III) oxide, iron metal and boron:

$$Fe_2O_3 + 4Fe + 8B \longrightarrow 6FeB + B_2O_3 \quad (III)$$
$$Fe_2O_3 + 4B \longrightarrow 2FeB + B_2O_3 \quad (IIIa)$$
$$Fe + B \longrightarrow FeB \quad (IIIb)$$

Table 1 Room-temperature X-ray and magnetic characteristics of FeM (M = B, Cr, VN and Ti) compounds produced by SHS in zero field. The parameters are maximum magnetisation σ_{max} (±0.01 emu g^{-1}) and remanent magnetisation σ_r (±0.01 emu g^{-1}) recorded in an external field of 10 kOe. The pycnometric densities d (g cm^{-3}) are also given.

Compound	σ_{max}	σ_r	d	Unit cell parameters/Å of SHS products a, b and c (±0.004 Å); V/Å^3 (±0.5 Å^3)	Reference X-ray data
FeB	61.90	3.55	4.9	a = 4.058 b = 5.510 c = 2.945 V = 65.85	a = 4.011 b = 5.470 c = 2.942 V = 64.55[7]
FeCr	16.30	0.97	5.8	a = 8.815 c = 4.505 V = 350.06	a = 8.800 c = 4.544 V = 351.89[8]
FeVN	2.03	0.52	5.2	a = 8.209 c = 4.562 V = 307.42	a = 8.943 c = 4.620 V = 369.49[9,a]
FeTi	0.42	0.04	5.2	a = 2.920 V = 24.90	a = 2.976 V = 26.36[10]

[a] Reference X-ray data for the FeV sample.

As found by SEM/EDAX and elemental analysis, all of the starting elements were distributed in the structure of SHS-prepared materials in an appropriate ratio. The EDAX spot analysis of the final products showed the expected Fe:M ratios without any additives. SEM showed micron-sized agglomerates of crystallites. X-ray analysis of all SHS samples showed that all of them were crystallised compounds which unit cell parameters are in full agreement with reference data (Table 1). The X-ray powder diffraction data for the SHS-prepared powders are consistent with that for materials prepared by conventional ceramic synthesis. Phase purity of all the samples was 92% or higher. The mean crystallite sizes d were calculated to be ~ 1000 Å for all the samples (except for FeCr) using the Sherrer equation. FeB exhibited an orthorhombic symmetry while FeCr and FeTi were tetragonal and cubic, respectively. Unfortunately, there are no reference data on the unit cell parameters of FeVN at room temperature. In comparison with the FeV lattice parameters, there is evidence about its tetragonal symmetry with some distortions, especially, along the a-axis, and an increase in the unit cell volume due to nitrogen insertion into the structure. The c/a parameter for FeV and FeVN were 0.517 and 0.555, respectively. The same structural transformations were reported for the different iron alloys with transition (Fe–Ta) and non-transition metals (Fe–Ge) after nitridation. All the SHS-prepared FeM compounds have lower maximum (σ_{max}) and remanent (σ_r) magnetisation values, as compared with appropriate amorphous compounds, and are soft magnetic materials like many other transition-metal alloys. The FeTi compound was reported to be paramagnetic in the bulk;[11] however, the SHS-

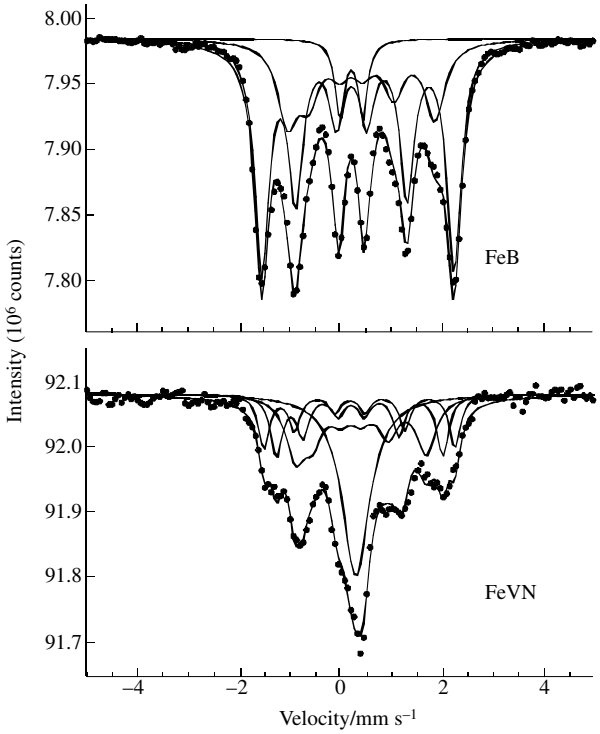

Figure 1 Room-temperature Mössbauer spectra of SHS-produced FeB and FeVN. The solid lines show the least-squares fit of the data.

prepared material exhibited a slightly ferromagnetic behaviour with a maximum magnetisation 0.42 emu g^{-1}.

Room-temperature transmission Mössbauer data were recorded on all four samples. FeB and FeVN gave magnetically split spectra (Figure 1), while FeTi gave a paramagnetic spectrum (Figure 2). Despite strenuous efforts, an unusable spectrum was obtained from FeCr because the extreme hardness of the material made it impossible to prepare a sufficiently thin Mössbauer absorber. The FeB, FeVN and FeTi spectra were analysed as a superposition of Lorentzian sextets, doublets and/or singlets, yielding the fit parameters given in Table 2.

The FeB spectrum was modelled as three magnetic sextets and one paramagnetic doublet. The majority phase component, accounting for 63% of the total spectral area, has a hyperfine field, $B_{hf} \approx 117$ kG, which is consistent with a reported value (118 kG) for stoichiometric crystalline FeB.[12–14] The second sextet, with its smaller B_{hf} and larger isomer shift δ, is probably due to some site disorder in the alloy, leading to Fe atoms encountering more than the usual number of near-neighbour interstitial B atoms. The minority phase doublet in the spectrum indicates that some Fe atoms are magnetically isolated in the sample.

The FeVN spectrum was best fitted to three sextets plus a singlet. The component sextets correspond to statistical variations

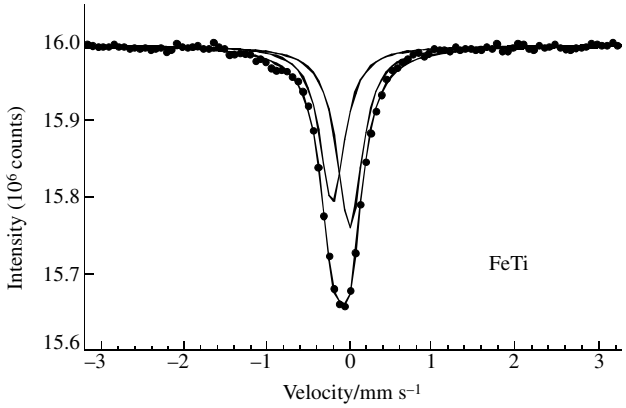

Figure 2 Room-temperature paramagnetic Mössbauer spectrum of SHS-produced FeTi.

Table 2 Room-temperature Mössbauer data for SHS-produced FeM (M = = B, VN and Ti) alloys. The parameters are the isomer shift δ, quadrupole shift 2ε or quadrupole splitting Δ, hyperfine field B_{hf}, and relative spectral area R of the subcomponent spectra.

Sample	δ/mms^{-1}	2ε or Δ/mms^{-1}	B_{hf}/kG	R (%)
FeB	0.28(1)	0.12(1)	117(2)	63(2)
	0.31(1)	0.20(2)	90(1)	30(2)
	0.22(1)	0.45(1)	—	7(1)
FeVN	0.28(2)	0.19(3)	116(2)	16(7)
	0.30(2)	0.17(3)	101(2)	20(11)
	0.30(2)	0.20(4)	80(3)	30(9)
	0.31(1)	—	—	34(4)
FeTi	–0.25(2)	—	—	46(10)
	–0.04(2)	—	—	54(10)

in the number of next-neighbour V and/or N atoms surrounding each Fe atom. Previous studies of FeAl alloys have shown three distinct sextets corresponding to 0, 3 and 4 next-neighbour Al atoms, with both the hyperfine field B_{hf} increasing and the isomer shift δ decreasing as the number of Al neighbours increased.[12,15,16] This trend in B_{hf} and δ is reflected in Table 2. The minority phase singlet also indicates that some Fe atoms are magnetically isolated in the sample. The paramagnetic FeTi spectrum was fitted as two singlets of approximately equal areas. The isomer shift of the left-hand singlet $\delta \approx -0.25$ mms^{-1} is close to the reported value (–0.26 mms^{-1}) for crystalline FeTi grown by arc melting.[17] The presence of a second singlet in the spectrum indicates some site disorder, perhaps leading to some more iron-rich regions with isomer shifts closer to zero.

References

1 S. Morris, S. B. Dodd, P. J. Hall, A. J. Mackinnon and L. E. A. Berlouis, *J. Alloys Compd.*, 1999, **295**, 458.
2 S. Tondu, T. Schnick, L. Pawlowski, B. Wielage, S. Steinhauser and L. Sabatier, *Surf. Coat. Technol.*, 2000, **123**, 247.
3 M. Xu, M. X. Quan, Z. Q. Hu and K. Y. He, *J. Mater. Sci. Technol.*, 2001, **17**, 260.
4 M. Jones, A. J. Horlock, P. H. Shipway, D. G. McCartney and J. V. Wood, *Wear*, 2001, **249**, 246.
5 A. D. Bratchikov, A. G. Merzhanov, V. I. Itin and V. M. Maslov, *Abstracts of II Conference on Technological Combustion*, Chernogolovka, Russia, 1978, p. 75 (in Russian).
6 L. Dalessio, R. Teghil, A. Santagata, V. Marotta, D. Ferro and G. DeMaria, *Surf. Coat. Technol.*, 1996, **80**, 221.
7 W. B. Pearson, *Handbook of Lattice Spacings and Structures of Metals*, Pergamon Press, Oxford, 1967.
8 JCPDS – International Centre for Diffraction Data, File 05-0708.
9 JCPDS – International Centre for Diffraction Data, File 07-0383.
10 JCPDS – International Centre for Diffraction Data, File 19-0636.
11 S. V. Mankovsky, A. A. Ostroukhov, V. M. Floka and V. T. Cherepin, *Vacuum*, 1997, **48**, 245.
12 N. N. Greenwood and T. C. Gibb, *Mössbauer Spectroscopy*, Chapman and Hall, London, 1971.
13 T. Shinjo, F. Itoh, H. Takaki, Y. Nakamura and N. Shikazono, *J. Phys. Soc. Jpn.*, 1964, **19**, 1252.
14 J. D. Cooper, T. C. Gibb, N. N. Greenwood and R. V. Parish, *Trans. Faraday Soc.*, 1964, **60**, 2097.
15 E. A. Friedman and W. J. Nicholson, *J. Appl. Phys.*, 1963, **34**, 1048.
16 M. B. Stearns and S. S. Wilson, *Phys. Rev. Lett.*, 1964, **13**, 313.
17 S. H. Liou and C. L. Chien, *J. Appl. Phys.*, 1984, **55**, 1820.

Received: 5th October 2001; Com. 01/1849